

KINETICS OF THE DEHYDRATION OF BOEHMITES PREPARED UNDER DIFFERENT HYDROTHERMAL CONDITIONS

TAKESHI TSUCHIDA, RYUSABURO FURUICHI and TADAO ISHII

Department of Applied Chemistry, Faculty of Engineering, Hokkaido University, Sapporo 060 (Japan)

(Received 20 November 1979)

ABSTRACT

The kinetics of the dehydration of five boehmites, which were prepared under different hydrothermal conditions (300°C, 85 atm, 20 h — 150°C, 4.5 atm, 5 h), were studied by means of isothermal TG at an air pressure of 150 mm Hg and at a constant flow rate of nitrogen (30 ml min⁻¹) containing water vapor of partial pressures between 10⁻⁴ and 23.8 mm Hg. It was found that the dehydration temperature of boehmites was lowered as the preparation conditions became more mild. Moreover, the rate-controlling step of the dehydration of boehmites varied with their preparation conditions. The water vapor pressure led to decreases in the rate of dehydration.

INTRODUCTION

The identification and characterization of various transition aluminas formed by the dehydration of boehmite, α -AlOOH, have been extensively investigated. Only a few papers [1–3], however, have been published on the kinetics and mechanism of the dehydration of boehmite, and they give conflicting results. Although it can be expected that the discrepancies between them are attributable to the differences in particle size, specific surface area and crystallinity of the boehmite used for the experiments, no detailed study has been reported.

The objective of the present study is to investigate systematically the influence of the preparation conditions of boehmites on the dehydration kinetics. The phase, crystallinity, crystallite size, specific surface area and reactivity of aluminas formed by the dehydration of boehmites have been described previously [4,5].

EXPERIMENTAL

Five boehmite samples were synthesized from bayerites under different hydrothermal conditions (shown in Table 1) in a SUS27 128 ml autoclave and sieved to obtain the -300 mesh fraction. The preparation of bayerite has been described previously [4]. Simultaneous TG-DTA or TG-DSC measurements were carried out using Rigaku Denki Model 8085 and 8076

TABLE 1

Preparation and properties of boehmites

Boehmite specimen	Hydrothermal conditions			Crystallite size D_{201} (Å)	Specific surface area ($\text{m}^2 \text{g}^{-1}$)	Water content * (wt%)	Heat of dehydration ** (kcal mole $^{-1}$)
	°C	atm	h				
(7)	300	85	20	1990	17	13.6	12.7
(8)	300	85	5	1260	19	13.6	12.8
(10)	200	16	20	860	33	14.2	10.7
(9)	200	16	5	480	63	14.1	10.1
(12)	150	4.5	5	260	109	14.3	8.3

* Amount of water dehydrated in the temperature range 200–600°C.

** Measured by the DSC method shown in Fig. 2.

thermoanalyzers under atmospheric pressure. Samples (6–10 mg) were heated to 600°C at a heating rate of 10°C min $^{-1}$ in DSC and to 1300°C at 20°C min $^{-1}$ in DTA. The heat of dehydration for the reaction



was measured by DSC. As shown in Fig. 2 curve (E), the heat of dehydration was determined from the shaded area bounded by the peak and the straight line connecting the two points at which it departed from the baseline. The calibration curve between peak area and heat was obtained by measurement of the heat of fusion or transition of KNO $_3$, In, Sn, Pb, Zn and Al. The weight loss values and the heats of dehydration are averages of at least five measurements.

The rate of dehydration of boehmite was determined with a Chan RG electrobalance by measuring the rate of decrease in sample weight due to the liberation of water vapor. The balance can detect a weight change of 10 $^{-6}$ g. Measurements at an air pressure of 150 mm Hg (static atmosphere) were carried out as follows. A sample of ca. 30 mg was packed into a small quartz bucket (ca. 0.4 ml) which was suspended from one arm of the balance and closed with a reaction tube of transparent quartz (i.d. = 32 mm, length = 600 mm). After the entire system had been evacuated with a vacuum pump for 30 min, air at 150 mm Hg was introduced into the reaction tube. Under these conditions, the water vapor pressure in the tube may be less than 2 mm Hg. When the furnace was controlled at a desired temperature, it was raised to the position of the sample. During the run, the weight of the sample was continuously recorded. The reaction temperature was between 398 and 479°C and was controlled within $\pm 1^\circ\text{C}$.

In order to investigate the effect of water vapor pressure on the rate of dehydration, the reactions were also carried out in dry or wet flowing (30 ml min $^{-1}$) nitrogen (a dynamic atmosphere). The nitrogen was passed through two gas-washing bottles filled with distilled water which were immersed in a constant-temperature bath (5, 15, or 25°C). Wet nitrogen saturated with water vapor of partial pressure (6.5, 12.8, or 23.8 mm Hg) was thus obtained. The dry nitrogen or the lowest vapor pressure was ob-

tained by passing nitrogen through two columns of activated alumina: the partial pressure of water was taken as $<10^{-4}$ mm Hg [6]. The nitrogen with a controlled vapor pressure was passed over the sample for 1 h before reaction. A double-walled reaction tube of quartz was designed for gas flow: i.d. of the inner and outer tubes = 29 and 38 mm, respectively. Dry nitrogen was counterflowed at 10 ml min^{-1} through an electrobalance to avoid the condensation of water vapor. The weight loss by dehydration was corrected by subtracting the apparent weight loss due to buoyancy which was previously measured with $\alpha\text{-Al}_2\text{O}_3$. All experiments in the dynamic atmosphere were carried out in the temperature range $405\text{--}477^\circ\text{C}$ and with a sample weight of ca. 15 mg.

The X-ray diffraction for boehmites and their dehydration products, i.e. transition alumina, was conducted with a Geigerflex 2141 type (Rigaku Denki Co.). The crystallite size was measured by X-ray line broadening using the Scherrer formula. The specific surface area was determined by measuring nitrogen adsorption at -196°C .

RESULTS AND DISCUSSION

Characterization of boehmites and their dehydration products

Table 1 shows the preparation conditions, crystallite size, specific surface area, water content and heat of dehydration of the boehmite samples. The water content was represented by the weight loss obtained in the temperature range $200\text{--}600^\circ\text{C}$, in which the adsorbed water was no longer contained. Further heating gave the weight loss of 1.3–1.8 wt.% in the temperature range $600\text{--}1300^\circ\text{C}$. It was found that when the preparation conditions of boehmite were more mild, the crystallite size was smaller and the specific surface area larger. A significant difference in the water content was not observed. The heat of dehydration decreased with milder preparation conditions of the boehmite sample. The heats of dehydration measured for boehmites (7) and (8) were in fair agreement with that ($12.6 \pm 1.1 \text{ kcal mole}^{-1}$) given by Yamada et al. [7] with a double-adiabatic high-temperature calorimeter.

Figure 1 shows the X-ray diffraction patterns for five boehmite samples. The diffraction lines for boehmites (7) and (8), which were prepared under the more severe hydrothermal conditions, are sharp and thus suggest a good crystallinity. The observed spacings and intensities of these lines are in fair accord with those in ASTM card 5-0190. On the other hand, when prepared under the milder conditions as boehmites (9) and (12), the diffraction lines became more diffused and of lower intensity, probably due to poor crystallinity. In addition, the intensity of the (150) and (002) lines was reversed.

Figure 2 shows TG–DSC curves for boehmite in the temperature range $200\text{--}600^\circ\text{C}$. When the boehmite was prepared under the milder conditions, the endotherm corresponding to dehydration was broadened and shifted to the lower temperature: the peak temperature was 521°C for boehmite (7) and 486°C for boehmite (12). This tendency agreed with that observed for

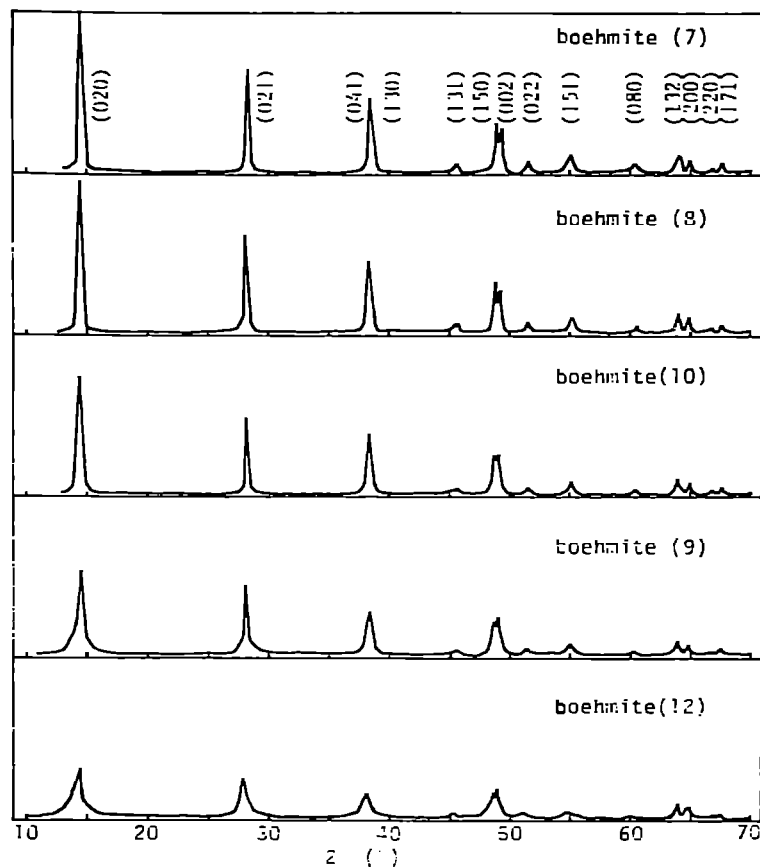


Fig. 1. X-Ray diffraction patterns of boehmites.

the initial temperatures of dehydration in the TG curves. Garn [8] pointed out that the peak temperature of dehydration depended on the size of the crystallites, because of either the higher stability of larger crystallites or the more difficult transport of gaseous products through longer narrow slits. A similar result was also obtained in the present experiments: the boehmite of the smaller crystallites and poor crystallinity showed the lower peak temperature of dehydration. It has already been reported [4] that the X-ray diffraction patterns of γ - Al_2O_3 as the dehydration product depended on the crystallinity of boehmite: the splitting of the (400) line of γ - Al_2O_3 obtained from well-crystallized boehmites (7) and (8) was very clear, but that of γ - Al_2O_3 from poorly crystallized boehmites (9) and (12) was obscure. In addition, these γ - Al_2O_3 samples had a different reactivity for the spinel formation with ZnO.

Table 2 shows the specific surface area of boehmites (S_1) and their dehydration products (S_2) which were obtained by the dehydration of boehmites at 250°C for 6 h and then at 500°C for 8 h. On dehydration, the specific surface area of products (S_2) increased. The ratio of the increase in the area (S_2/S_1) tended to be smaller for the poorly crystallized boehmites. This is in agreement with that reported by Lippens and Steggerda [9] who

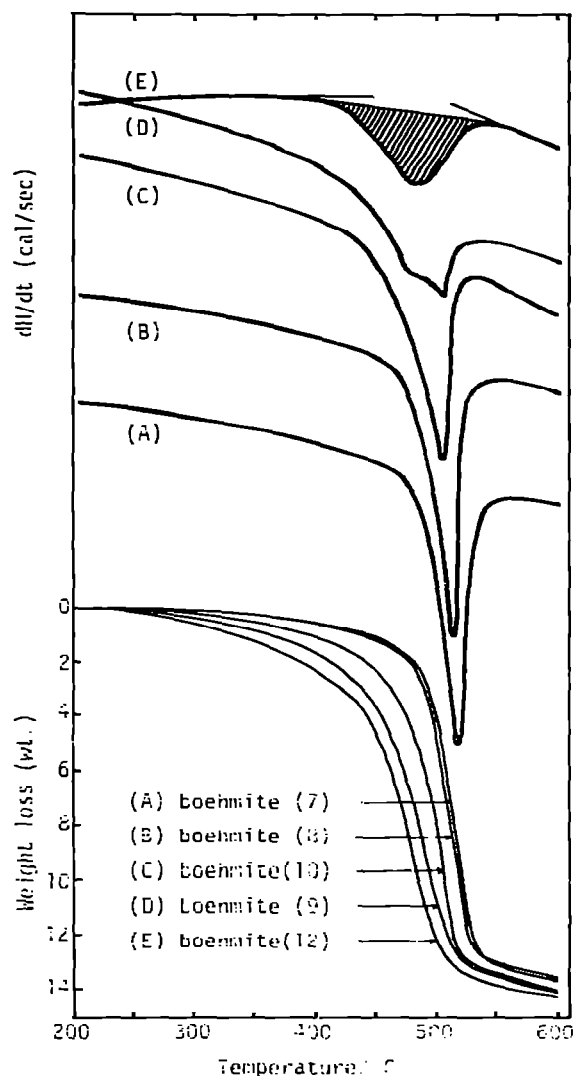


Fig. 2. TG—DSC curves for boehmites. $\phi = 10^{\circ}\text{C min}^{-1}$, in static air. Heat of dehydration is determined from the shaded peak area in DSC curve (E).

TABLE 2

The specific surface area of boehmites and their dehydration products ($\text{m}^2 \text{g}^{-1}$)

Boehmite specimen	Dried at 130°C (S_1)	Dehydrated at 250°C for 6 h and then at 500°C for 8 h (S_2)	Increase (S_2/S_1)
(7)	17	51	3.0
(8)	19	67	3.5
(10)	33	67	2.0
(9)	63	96	1.5
(12)	109	148	1.4

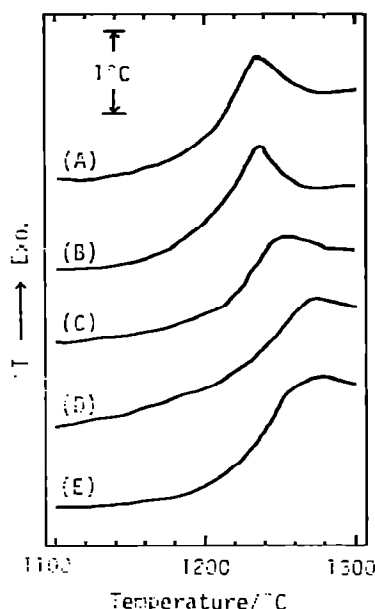


Fig. 3. DTA curves for boehmite to α - Al_2O_3 transformation. $\phi = 20^\circ\text{C min}^{-1}$, in static air. (A), (B), (C), (D), (E): boehmite (7), (8), (10), (9) and (12), respectively.

pointed out that on heating well-crystallized boehmite, the pores smaller than 20 \AA were produced by the loss of water, causing an increase in surface area, while in the case of poorly crystalline boehmite or pseudoboehmite, the loss of surface area resulted from a shrinkage of the particles and an absence of new micropores.

Figure 3 shows the DTA curves of boehmites in the temperature range 1100 – 1300°C . As has been previously shown [5], the boehmite transformed according to



The baseline of the DTA curves began to shift to the exothermic side at a temperature above 1100°C and the peak of transformation to $\alpha\text{-Al}_2\text{O}_3$ appeared between 1230 and 1270°C . The lower peak temperature was observed for the boehmites prepared under the more severe conditions: 1237°C for boehmite (7) and 1270°C for boehmite (12). These results also agree with those obtained in the isothermal experiments at 1100°C for 2 h [5]. This fact can be ascribed to the good crystallinity of transition aluminas obtained from well-crystallized boehmite, which is favorable for the α -transformation accompanying the crystal growth.

Kinetics and mechanism of dehydration

The isothermal dehydration of boehmites prepared under different hydrothermal conditions was studied in various atmospheres. The experimental results were tested by a reduced-time method proposed by Sharp et al. [10] which was based on the time for 50% reaction (α vs. $t/t_{0.5}$), and compared

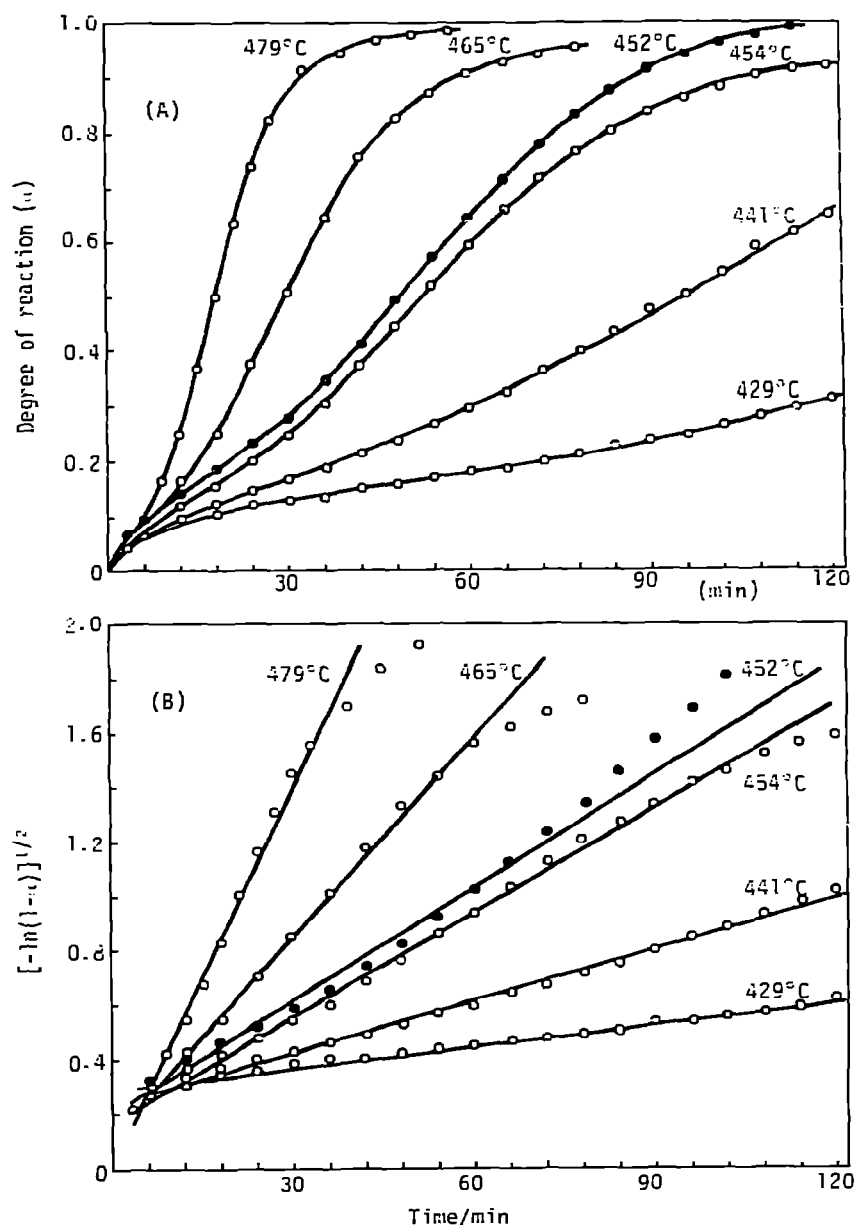


Fig. 4. Dehydration of boehmite (7), \circ , and boehmite (8), \bullet , at an air pressure of 150 mm Hg. (A) α vs. time; (B) $A_2(\alpha)$ (from the Avrami-Erofeev equation) vs. time.

with master curves for various model systems. Consequently, it was found that the rate-controlling step of the dehydration of boehmites varied with their preparation conditions.

Figures 4–6 show the rate curves for the dehydration for various boehmites at an air pressure of 150 mm Hg. The degree of reaction (α) was represented by the fraction of the amount of water dehydrated at a given temperature and the time taken to achieve the water content shown in Table 1. Figure 4(A) shows the rate curves of boehmites (7) and (8) pre-

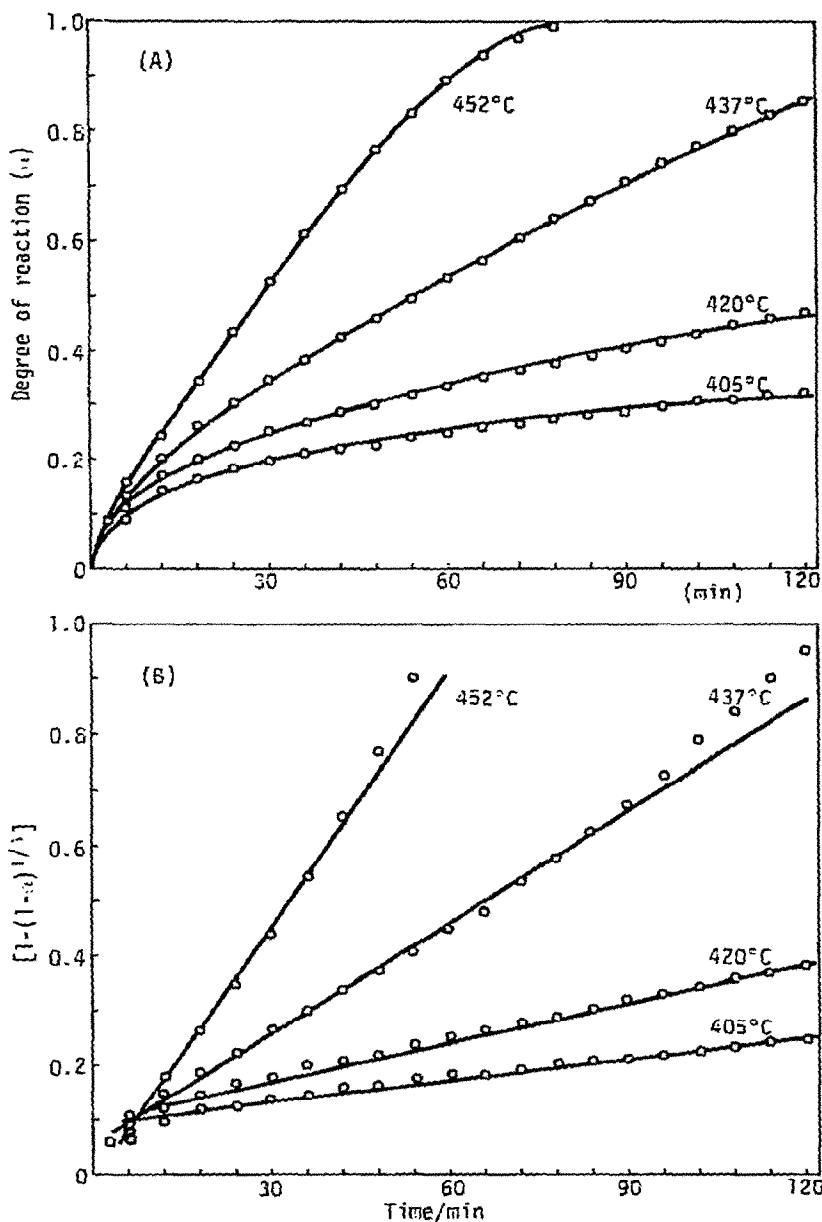


Fig. 5. Dehydration of boehmite (10) at an air pressure of 150 mm Hg. (A) α vs. time; (B) $R_3(\alpha)$ (from the contracting volume equation) vs. time.

pared under the more severe conditions. In the range of α from 0.1 to 0.9, the data shown in Fig. 4(A) fitted well the Avrami-Erofeev equation, $A_2(\alpha)$, as shown in Fig. 4(B)

$$A_2(\alpha) = [-\ln(1-\alpha)]^{1/2} = kt \quad (2)$$

This equation was derived on the basis that nucleation is a rate-controlling process. Not all the experimental data for boehmite (8) are included in Fig. 4 for the sake of clarity, but they also fitted $A_2(\alpha)$. From comparison of the data for boehmite (7) at 454°C with those for boehmite (8) at 452°C, it

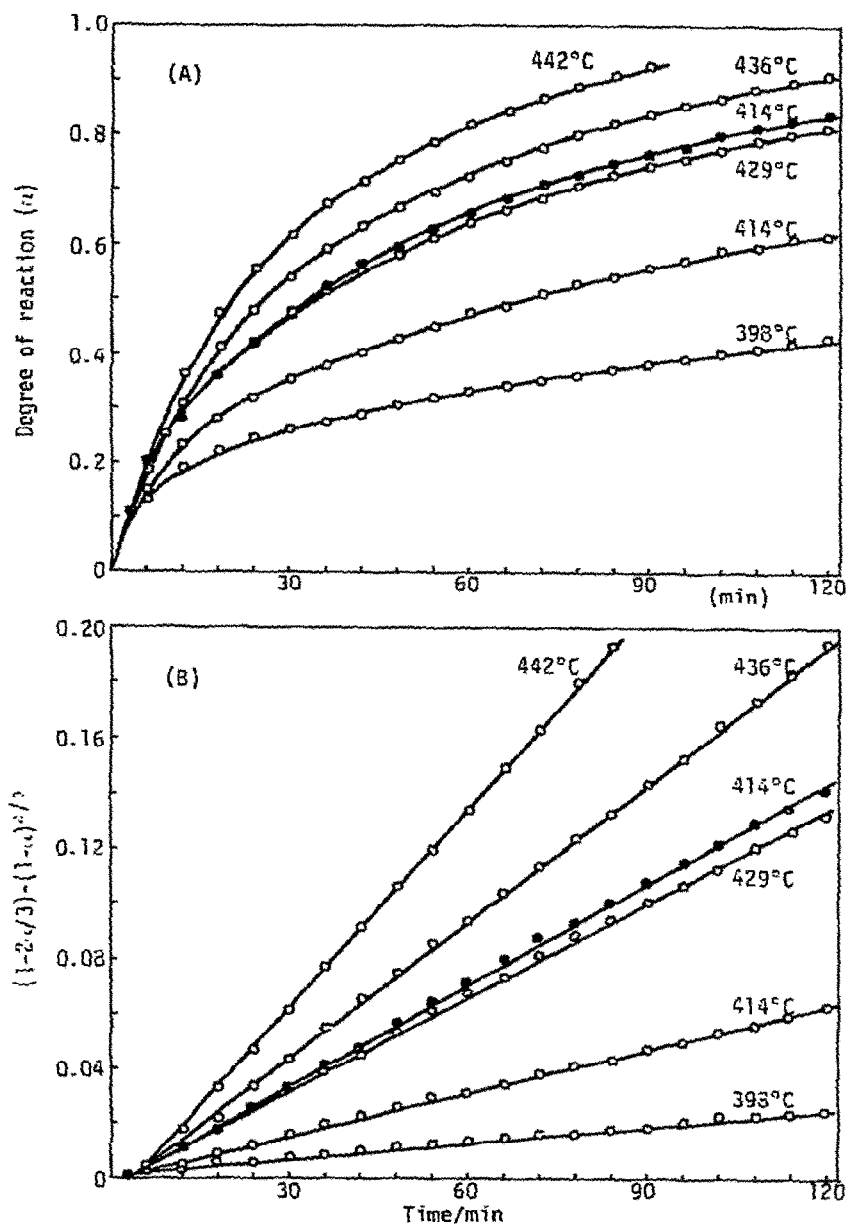


Fig. 6. Dehydration of boehmite (9), \circ , and boehmite (12), \bullet , at an air pressure of 150 mm Hg. (A) α vs. time; (B) $D_4(\alpha)$ (from the Ginstling-Brounshtein equation) vs. time.

was observed that the latter gave the somewhat higher α values in spite of a lower reaction temperature by 2°C . This may be due to the milder preparation conditions for boehmite (8) than those for boehmite (7).

Figure 5(A) shows the rate curve for boehmite (10). The reaction temperatures, in general, were lower by ca. 20°C than those for boehmites (7) and (8). As shown in Fig. 5(B), the data fitted the equation of phase-boundary controlled reaction for spherical particles, $R_3(\alpha)$, in the α range 0.1–0.8

$$R_3(\alpha) = [1 - (1 - \alpha)^{1/3}] = kt \quad (3)$$

TABLE 3

Activation energies (kcal mole⁻¹) under various atmospheres

Boehmite specimen	Static atmosphere air pressure (150 mm Hg)	Dynamic atmosphere (30 ml min ⁻¹) water vapor pressure (mm Hg)			
		<10 ⁻⁴	6.5	12.8	23.8
(7)	59	69	78	78	78
(8)	65				
(10)	54	62	63	60	62
(9)	53	54	58	57	56
(12)	53				

Figure 6(A) shows the results for boehmites (9) and (12) prepared under the milder conditions. The reaction temperatures were somewhat lower than those for boehmite (10). One set of data for boehmite (12) is represented in Fig. 6 for the sake of clarity. As shown in Fig. 6(B), the results in Fig. 6(A) fitted best the Ginstling—Brounshtein equation of diffusion control, $D_2(\alpha)$, up to 100%

$$D_2(\alpha) = (1 - 2\alpha/3) - (1 - \alpha)^{2/3} = kt \quad (4)$$

As can be seen from a comparison of the data for boehmite (9) at 429°C with those for boehmite (12) at 414°C, the latter obtained under the milder preparation conditions gave the higher rate of dehydration. The Arrhenius plots for the rate constants obtained in all boehmite systems gave the activation energies, 53–65 kcal mole⁻¹, shown in the first column of Table 3.

Next, the effect of water vapor pressure on the rate of dehydration was investigated. Figure 7 shows an example of the results for boehmites (7), (10) and (9) which were measured in dynamic atmospheres, i.e. in dry (water vapor pressure, <10⁻⁴ mm Hg) and wet nitrogen (23.8 mm Hg) at a flow rate of 30 ml min⁻¹. A comparison of the rates obtained for the same boehmite shown in Fig. 7 and Figs. 4–6 indicates that a static air pressure of 150 mm Hg gives a somewhat faster rate than dynamic dry nitrogen. This is presumably due to the difference in the total pressure. As can be seen from Fig. 7, the water vapor pressure led to remarkable decreases in the rates of dehydration for all boehmites, in spite of the discrepancy in the reaction temperatures. This can be interpreted by the decrease in the effective reaction surface due to chemisorption of water on the boehmite surface [11]. The experiments were also carried out at other vapor pressures, i.e. 6.5 and 12.8 mm Hg. Consequently, it was found that the same rate equation was applicable to data measured in dynamic atmospheres, i.e. water vapor did not alter the rate-controlling step of the dehydration reaction. Arrhenius plots of the rate constants obtained in dynamic atmospheres are shown in Fig. 8 and the activation energies in Table 3. The water vapor pressure caused the rate constant to decrease, but the variation of the water vapor pressure used in these experiments had little effect on the rate constant. The

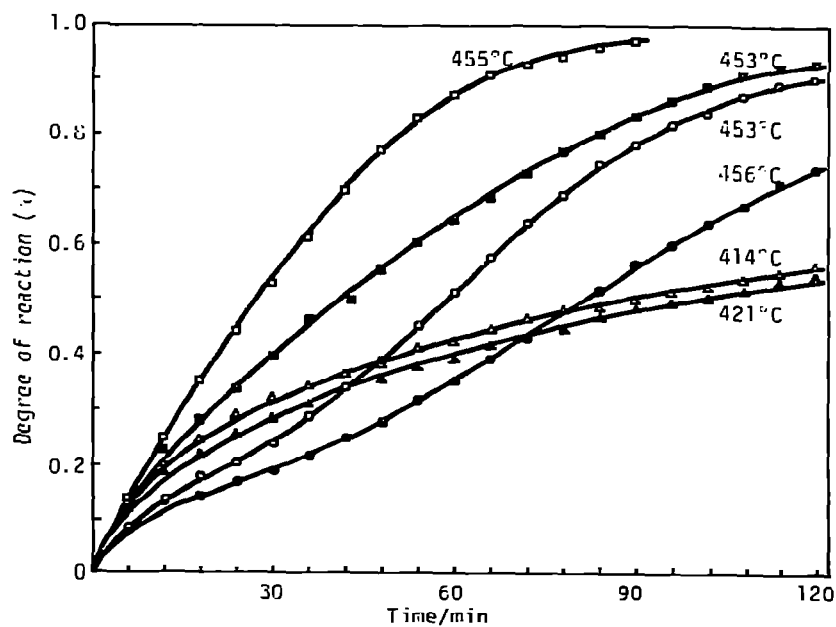


Fig. 7. Effect of water vapor pressure on the dehydration of boehmite (7) \circ, \bullet ; boehmite (10) \square, \blacksquare ; and boehmite (9) $\triangle, \blacktriangle, \circ, \square, \triangle, \blacktriangle$, $<10^{-4}$ mm Hg; $\bullet, \blacksquare, \blacktriangle$, 23.8 mm Hg.

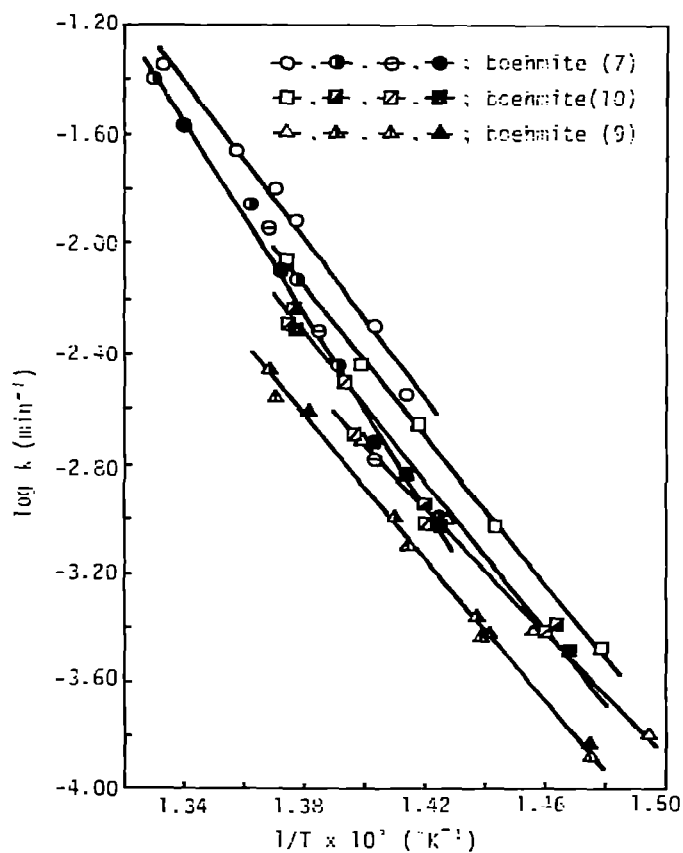


Fig. 8. Effect of water vapor pressure on $\log k$ vs. $1/T$ plots. $\circ, \square, \triangle$, $<10^{-4}$ mm Hg; $\circ, \square, \triangle$, 6.5 mm Hg; $\circ, \square, \triangle$, 12.8 mm Hg; $\bullet, \blacksquare, \blacktriangle$, 23.8 mm Hg.

activation energies obtained in dynamic atmospheres were somewhat larger than those in a static one, and were also insensitive to the variation of the water vapor pressure.

From the above results, it was found that the dehydration reaction of boehmite was extremely complex and that the different reaction steps, i.e. nucleation-, phase boundary- and diffusion-control, were rate-controlling under varying preparation conditions of boehmites. The variation in the kinetics may depend not only on the physical state of the reactants, but also on that of the products. A possible mechanism for the dehydration of boehmite can be suggested as follows. The model includes the sequences of individual steps. Initially, the nucleation of products occurs at active sites on the boehmite surface. As the nuclei grow larger, they overlap each other and then the surface of each boehmite particle is covered with a continuous product layer through which the water molecules diffuse. When the diffusion of water molecules through the product layer is so rapid, the reaction is phase-boundary controlled. Therefore, the kinetics of the dehydration of boehmite depend on which step is rate-controlled. The well-crystallized boehmites (7) and (8) have presumably less structural imperfections and less active sites as potential nucleation sites, and thus their dehydration was a nucleation-controlled reaction. On the other hand, it is considered that the poorly crystalline boehmites (10), (9) and (12) prepared under the milder conditions have many imperfections and active sites. Therefore, the nucleation step occurs instantaneously, so that the surface of each particle is covered with a product layer. Then, the fact that the rate-controlling step in the dehydration of boehmites (9) and (12) was diffusion-controlled should be accounted for on the basis of the formation of the compact and impermeable layer of the product. Such a nature of the product layer depends strongly on the pore structure. In general, because the molar volume of product is smaller than that of reactant in thermal decomposition, the product layer is formed from the aggregation of fine particles, and thus contains enough micropores and cracks to escape water vapor. However, in the case of the dehydration of boehmite, the quantity of new pores produced by the dehydration depended on the crystallinity of boehmite. As shown in Table 2, the degree of increase in specific surface area (S_2/S_1) by dehydration was larger for well-crystallized boehmites. This suggests that the product layer does not impede the diffusion of water outside the particles. On the other hand, the smaller values of S_2/S_1 for poor crystalline boehmites prepared under the milder conditions imply that the product layer is relatively compact and impervious.

ACKNOWLEDGEMENT

The authors are sincerely grateful to Dr. T. Okutani for use of the TG—DTA/DSC thermoanalyzer.

REFERENCES

- 1 C. Eyraud and R. Goton, *J. Chim. Phys.*, 51 (1954) 430.
- 2 W.D. Callister, I.B. Cutler and R.S. Gordon, *J. Am. Ceram. Soc.*, 49 (1966) 419.
- 3 L. Abrams and M.J.D. Low, *I EC Prod. Res. Dev.*, 8 (1969) 38.
- 4 T. Tsuchida, R. Furuichi and T. Ishii, *Z. Anorg. Allg. Chem.*, 415 (1975) 175.
- 5 T. Tsuchida, R. Furuichi and T. Ishii, *Z. Anorg. Allg. Chem.*, 423 (1976) 180.
- 6 R.E. Dodd and P.L. Robinson, *Experimental Inorganic Chemistry*, Elsevier, Amsterdam, 1957, p. 137.
- 7 K. Yamada, F. Fukunaga, Y. Takahashi and T. Mukaibo. *J. Electrochem. Jpn.*, 41 (1973) 290.
- 8 P.D. Garn, *Thermoanalytical Methods of Investigation*, Academic Press, New York, 1965, p. 95.
- 9 B.C. Lippens and J.J. Steggerda. in B.G. Linsen (Ed.), *Physical and Chemical Aspects of Adsorbents and Catalysts*, Academic Press, London, 1970, p. 194.
- 10 J.H. Sharp, G.W. Brindley and B.N.N. Achar, *J. Am. Ceram. Soc.*, 49 (1966) 379.
- 11 G.W. Brindley, J.H. Sharp, J.H. Patterson and B.N.N. Achar, *Am. Mineral.*, 52 (1967) 201.